# Advanced human 3D-bioprinted skin constructs to model inflamm'aging

Vert Laure[1], Franchi Jocelyne[1], Pecher Virginie[1], Choisy Patrick[1], Jeanneton Olivier[1], Albouy Marion[2], Dos Santos Morgan[2], Thepot Amelie[2], Capallere Christophe[3], Imbert Isabelle[3], **Nizard Carine**[1*]

[1]LVMH RECHERCHE, 45804 Saint Jean de Braye, France ; [2]Labskin Creations, 69437 Lyon, France; [3]Ashland, 06904 Sophia Antipolis, France

٭ Corresponding author/ Nizard Carine, 185 Av. de Verdun, 45800 Saint-Jean-de-Braye +33238603406, cnizard@research.lvmh-pc.com

## Abstract

**Background**: Throughout its life, human skin is constantly undergoing aggression from different origins, which cumulatively adds to its physiological aging. Exposed daily to these various physical or chemical stimuli, an inflammatory-like response can be triggered for the skin to efficiently resist and protect itself. The term inflamm'aging reflects this close relationship between inflammation and aging. While we gained a lot of insights on the molecular mechanisms driving inflamm'aging using 2D cellular models, a more integrated view is needed to grasp both molecular and cellular consequences on human skin.

**Methods**: Here, we used predictive 3D skin models to mimic inflamm'aging using UV radiation and assessed its consequences at the cellular and tissular level. We also tested a new advanced eco-extraction of Granville Rose (GR) with a process of magnetic waves and centrifugation and assessed its effect on all skin layers.

**Results**: We found that a combination of UVA and UVB disorganized fibrillin-1 fiber network, but that a treatment of skin biopsies with GR extract prevented these deleterious effects on skin dermal structure. Using a 3D bioprinted human skin model of inflamm'aging, we could further show that GR extract protected from skin epidermal thinning induced by chronic UVA exposure, as well as from the decreased expression of filaggrin. In the dermal compartment, extracellular matrix density was improved, and the expression of collagen III restored.

**Conclusion**: Altogether, our results point to a protection effect of GR extract on an advanced skin model of inflamm'aging.

**Introduction**

Skin is the largest organ of the human body, but also the one organ directly exposed to the external environment. Throughout its life, human skin is constantly undergoing aggression from different origins, which cumulatively adds to its physiological aging [1,2]. Exposed daily to these various physical or chemical stimuli, an inflammatory-like response can be triggered for the skin to efficiently resist and protect itself. However, the skin becomes more fragile, and several essential features are less efficient: the skin's epidermal hydrolipid film becomes poorer, the intracellular cement does not properly perform its barrier function, opening the door to dehydration. The dermis becomes thinner, with elastic fiber degradation, fragmented collagen fibers, and dermal connective tissue damage. The term inflamm'aging reflects this close relationship between inflammation and aging, concept that originated in the 20's with the "inflammation hypothesis of aging" [3,4].

Micro-inflamed skin displays the classic signs of inflammation that are not immediately visible, the so-called silent or sterile inflammation. Specific mediators of inflammation are produced in small amounts within the skin by cells that are exposed to their environment or in response to their own metabolism. It is the repetition, chronicity, accumulation that eventually alter the physiological balance of the skin leading to a loss of functionality and the appearance of visible aging signs [5]. Importantly, all skin layers are affected by inflamm'aging, as the expression of mediators of inflammation will impact the epidermis structure, its barrier function, and dermal integrity. As a first line of defense, keratinocytes within the epidermis act as true stress sensors, locally initiating the production of known mediators of inflammation. They release lipid mediators such as PGE2, and protein mediators such as cytokines [6].

One of the key elements that favors inflamm'aging is the chronic exposure to ultraviolet radiation (UVR), naturally emitted from the sun and artificial sources. Some wavelengths from sunlight such as UVC (100-280 nm) are absorbed by the ozone layer and have little impact on human skin. However, some UVB (280-320 nm) can penetrate the skin epidermis, while UVA (320-400 nm) can reach deeper in the skin dermis and induce premature skin aging in part through an inflammatory response [7]. The chronicity of the inflammatory state is intimately linked to oxidative stress via the generation of free radicals and reactive oxygen species (ROS). The targets are numerous as well as the consequences, such as a depletion of antioxidants and antioxidants

enzymes, initiation of DNA damage, and the release of proteases that will target the extracellular matrix (ECM) [8].

While we gained a lot of insights on the molecular mechanisms driving inflamm'aging using 2D cellular models, a more integrated view is needed to grasp molecular and cellular consequences on human skin at both cellular and tissular levels. Here, we intended to mimic inflamm'aging on various predictive 3D skin models. We also tested a new advanced eco-extraction of Granville Rose (GR) with a process of magnetic waves and centrifugation and assessed its effect on all skin layers.

## Materials and Methods

### Ex-vivo skin biopsies

Normal human skin biopsies came from plastic surgery intervention on the abdomen of donors aged from 26 to 66-years old. Skin biopsies were obtained with a 6-mm punch and were kept in culture medium containing 50%/50% DMEM 1g/l glucose and Ham's-F12 medium, supplemented with 10% fetal bovine serum, 2mM L-glutamine, and 100 µg/ml Primocin. Skin biopsies were maintained at 37°C in a humidified atmosphere containing 5% $CO_2$. When indicated, skin biopsies were treated with GR extract at 0.3% in PBS twice a day for 48h, or with PBS as a control. Biopsies were or not subjected to 5J/cm$^2$ UVA followed by 200mJ/cm$^2$ UVB after the first 24h of treatment with the active.

Fibrillin-1 staining on skin biopsies

Tissues were frozen in OCT medium using liquid nitrogen and conserved at -20°C. Frozen skin biopsies were then cut with a cryotome into 6 µm thick sections and placed on glass slides before staining. Skin sections were dried for 30min at 37°C, fixed in cold acetone for 10min and rinsed in PBS. Non-specific sites were saturated with 5% BSA, following antibody incubation and DAPI staining. Slides were detected with a Nikon Eclipse Ni-E microscope and processed with the manufacturer's software. Image quantification was performed with ImageJ software. The total length of the selected fibers was measured and normalized by the length of the dermal epidermal junction. Five images per condition were analyzed. Final quantification represents the average of 2 independent experiments (n=12).

**3D bioprinted full-thickness skin model culture**

Primary cultures of normal human dermal fibroblasts (NHDF) and epidermal keratinocytes (NHEK) and melanocytes (NHEM) were established from healthy skin biopsies obtained from infant donor (under 5 years old) undergoing plastic surgery, according to the French regulation including declaration to the research ministry (DC No. 2020-4346).

3D bioprinted full-thickness skin model was engineered in 2 steps. The dermal equivalent constructs have been produced according to a scaffold-free approach by self-assembly method. The dermal tissues were enabled to produce their own extracellular matrix for three weeks at 37◦C and 5% $CO_2$. After this time frame, NHEK and NHEM were inkjet printed on the dermal construct, at a density of 10,000 cells/cm2 in a precise and optimized arrangement and geometries without any carrier. After 72 hours of submerged culture, 3D bioprinted constructs were raised at the air–liquid interface to allow epidermal differentiation. GR extract at 0.1% or 0.2% was added to 3D skin models from day 14 to the end of culture. From day 42, the constructs were irradiated with UVA 12J/cm2 for 6 days or 16 J/cm2 for 3 days. Samples were systematically harvested and fixed for histological and immunohistological analysis. Supernatants were collected at the end of the total cell culture for biochemical analysis.

Histological analysis

Paraffin-embedded formalin-fixed samples were then cut into 5μm sections. After dewaxing and rehydration, sections were stained with Hematoxylin–Phloxin–Saffron for routine histology.

Immunohistological analysis

Immunostaining was performed on paraffin-embedded formalin-fixed samples of 5μm. After dewaxing and antigenic unmasking, the sections were incubated with PBS containing 5% BSA to block non-specific antigenic bonds. The sections were then incubated with the primary antibody anti-filaggrin and collagen III. A secondary antibody conjugated to Alexa-568 was incubated for 1 hour at room temperature. Nuclear counterstaining using Hoechst was carried out systematically.

Image acquisition and analysis

Specimens stained in HPS were observed using an Axioskop 2 Plus optical microscope (Zeiss), and images were captured using DS-Ri1 CCD camera (Nikon) and NIS-Elements software (Nikon). Sixteen-bit images were saved in an uncompressed tagged image file format (tiff). Six representative images were captured for each condition in the same manner. Image processing and analysis were performed using the software MBF_ImageJ for microscopy. The parameters in which

we were interested were the epidermal thickness for HPS- stained sections and the positive surface area for filaggrin and type III collagen.

*Epidermal thickness:* Epidermal thickness was obtained with a Euclidean distance map. Pixels corresponding to the epidermis were selected from other pixels. Images were converted to 8-bit binary image. Images corresponding to the area of interest were converted to a 16-bit distance map. To each epidermis pixel (nonzero) in the distance map binary image a value equal to its distance from the nearest background pixel (zero) was assigned. The epidermis basal line was selected and then applied on the distance map. The mean intensity of the basal line corresponds to the mean distance between the basal line and the *stratum corneum*. Data are expressed in μm.

*Surface measurement:* positively stained-tissue areas were automatically detected and segmented from other pixels. Images were then converted in binary images, treated by mathematical morphology and sieved for isolating the regions of interest. The surface area of interest was measured automatically. Data were normalized by the length of basement membrane, the total epidermal or dermal surface and results were expressed in pixel$^2$ per μm.

TEWL evaluation on 3D bioprinted skin model

Transepidermal water loss was measured by using noninvasive techniques using closed-chamber instrument.

**Statistical analysis**

Statistical analyses were performed using Student's t-test. **** $p < 0.0001$, *** $p < 0.001$, **$p < 0.01$, * $p < 0.05$
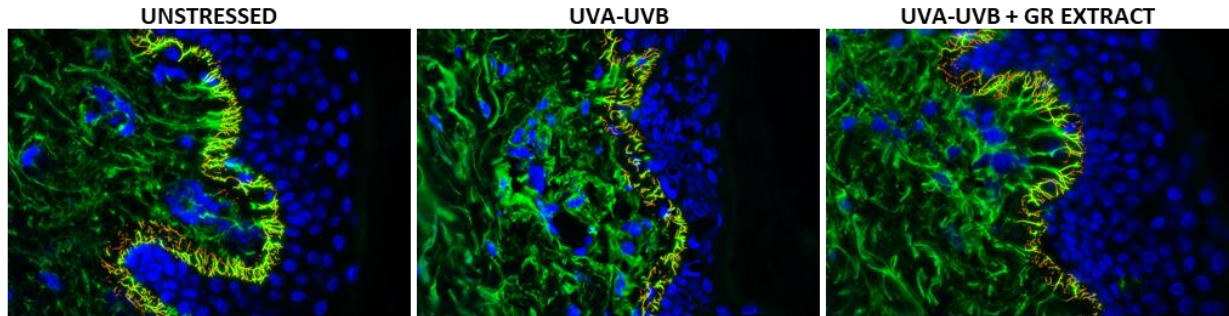
**Results**

**A combination of UVA and UVB induces fibrillin degradation that is improved upon GR extract treatment.**

We first used skin biopsies stressed with 5 J·cm$^{-2}$ UVA followed by 200 J·cm$^{-2}$ UVB to assess the impact on the skin dermal compartment. Fibrillin-1, one key structural component of the skin dermal elastic fiber network was visualized by immunostaining. After 48 hours, UVR impacted the fibrillin-1 organization, with a 17% decrease of their total length (Figure 1A-B). When skin biopsies were treated with GR extract however, fibrillin fibers were protected from UVR as we

observed an increase of 13% in fiber length (Figure 1A-B). This result highlights the capacity of GR extract to prevent deleterious effects of UVR on skin dermal structure, as changes in the ECM composition will affect cellular activities and tissue properties [9].
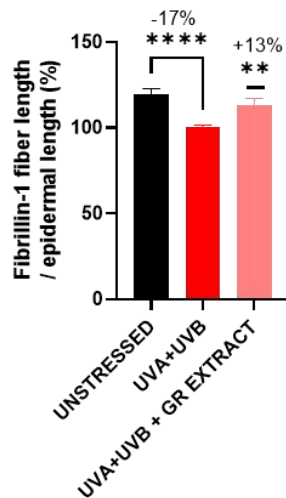


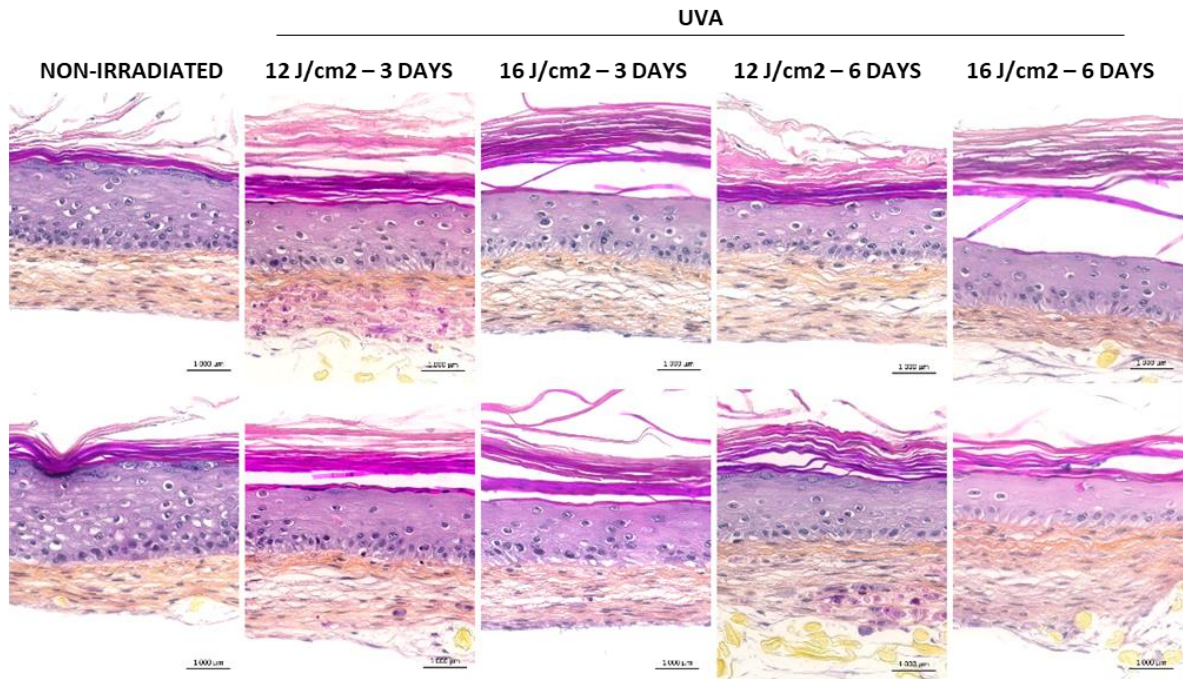FIGURE 1: GR extract prevents UVA+UVB-induced fibrillin degradation
A- Representative images of fibrillin-1 immunostaining of human skin biopsie sections: DAPI (blue), Fibrillin-1 (green). Fiber network skeleton is highlighted in yellow-red by computer-assisted image processing. Images were acquired with a 40x objective.
B- Quantification of A. The percentage of fibrillin fiber length relative to epidermal length is shown (means +/- SEM; n=12).

**Chronic UVA treatment to model inflamm'agin**

Next, we established a reconstructed human skin model of inflamm'aging. Dermal equivalents were produced by using scaffold-free self-assembly method of human normal skin fibroblasts, on top of which human normal keratinocytes were seeded. Reconstructed skin samples displayed a thick and pluristratified epidermis supported by a dermal compartment dense in neosynthesized ECM (Figure 2A, non-irradiated condition). To set the experimental conditions of irradiation, samples were irradiated with 12 or 16 J·cm$^{-2}$ UVA for 3 or 6 days. Compared to unirradiated controls, UVA treatment strongly affected the epidermal barrier function, with a marked increase of the measured TEWL.
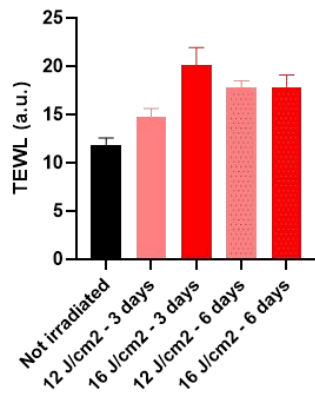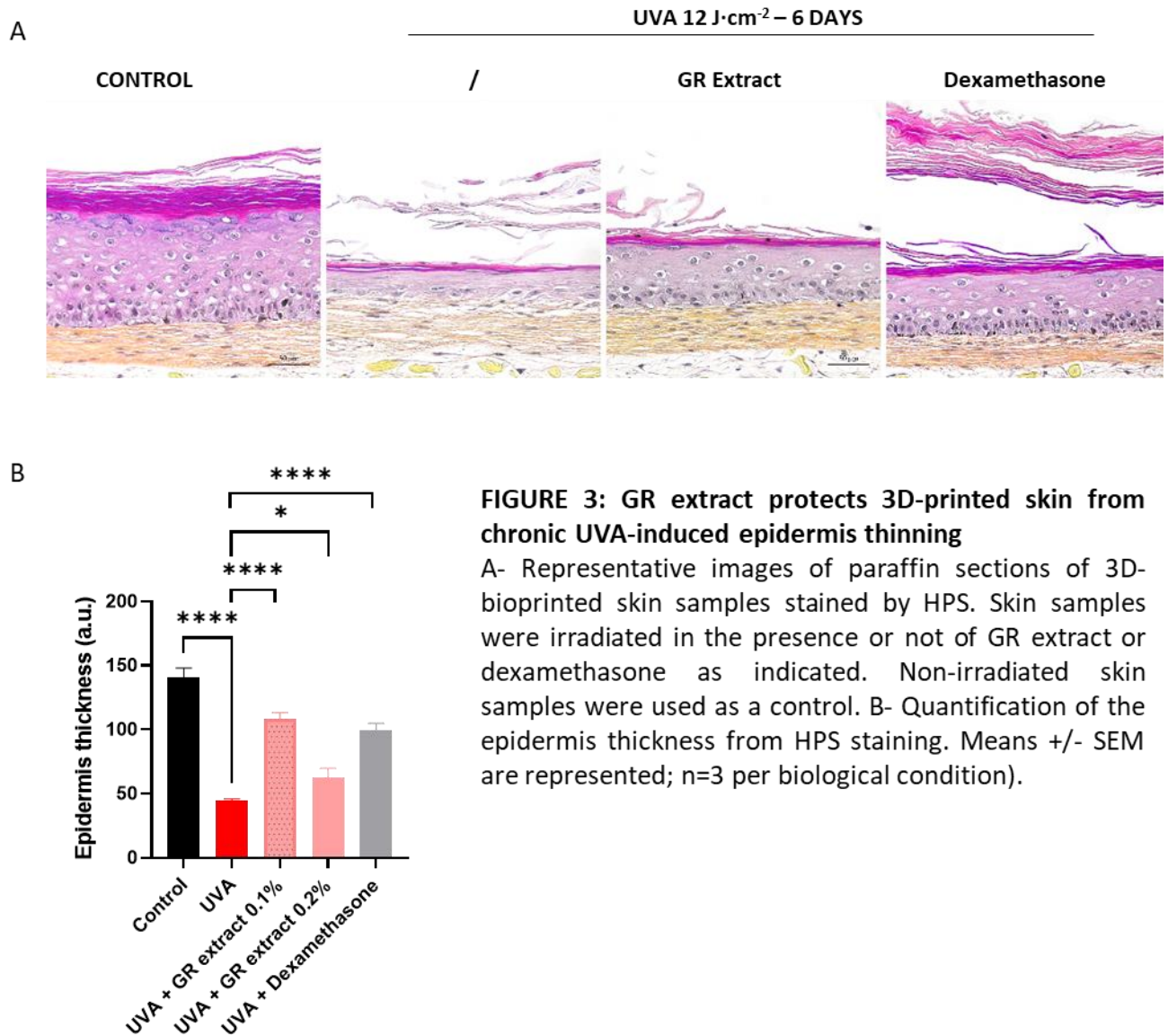
A



B



**FIGURE 2: Set-up of irradiation conditions for chronic inflammation**
A- Representative images of paraffin sections of 3D-bioprinted skin samples stained by HPS, with or without UVA irradiation as indicated. B- Quantification of the Transepidermal Water Loss (TEWL). Means +/- SEM are represented; n=3 per biological condition).

This result correlated with a disorganized epidermal basal layer, and impaired dermal structure that appeared less dense after irradiation (Figure 2A-B). A dose-dependent response was observed, as well as a stronger phenotype after 6 days compared to 3 days for the lower UVA treatment used. These results prompted us to validate the dose of 12 J·cm$^{-2}$ of UVA chronically applied to mimic inflamm'aging in subsequent experiments.

**GR extract protects 3D bioprinted skin from chronic UVA-induced epidermis thinning**

Dermal equivalents were produced by using scaffold-free self-assembly method as before, but we used the bioprinting technology to generate the epidermal layer. Epidermis bioprinting was performed using an inkjet bioprinter equipped with a piezoelectric nozzle. An optimized design bioprinting pattern was used to bring the best results in term of epidermis homogeneity and reproducibility. GR extract was added by systemic treatment from the dermal maturation until the bioprinting of the epidermal layers, as well as during the chronic UVA treatment up to 42 days.



**FIGURE 3: GR extract protects 3D-printed skin from chronic UVA-induced epidermis thinning**
A- Representative images of paraffin sections of 3D-bioprinted skin samples stained by HPS. Skin samples were irradiated in the presence or not of GR extract or dexamethasone as indicated. Non-irradiated skin samples were used as a control. B- Quantification of the epidermis thickness from HPS staining. Means +/- SEM are represented; n=3 per biological condition).

First, several morphological parameters were analyzed. Chronic UVA irradiation strongly affected skin morphology, with a thin, disorganized epidermis, and a defect in epidermal differentiation (Figure 3A-B). The dermal compartment was also impacted, with a decrease in synthesized ECM.

Systemic treatment with GR extract rescued all these phenotypes. Despite chronic irradiation, epidermis thickness was increased by 145% with 0.1% GR extract compared to UVA-treated alone. Remarkably, GR extract protective action was comparable to treatment with dexamethasone, a pharmacologic drug known for its anti-inflammation properties (Figure 3).

**GR extract protects epidermal differentiation from chronic UVA stress**

Next, we performed immunostaining to evaluate the effect of inflamm'aging on epidermal features and the property of GR extract to prevent its deleterious consequences. We stained for filaggrin, which plays a leading role in the process of keratinocyte differentiation to ensure a proper barrier formation (Figure 4A).
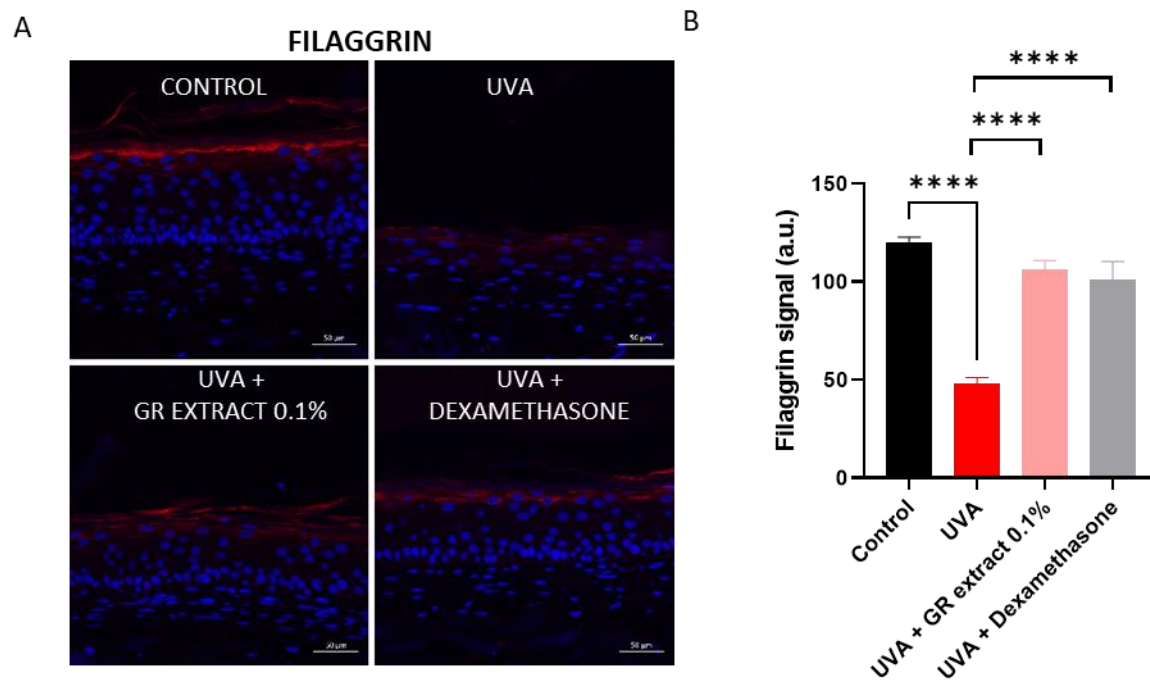


**FIGURE 4: GR extract protects 3D-printed skin from chronic UVA-induced decrease in filaggrin expression**

A- Representative immunostaining of 3D-bioprinted skin samples stained with antibodies against Filaggrin in red and stained with DAPI in blue. Skin samples were irradiated in the presence or not of GR extract or dexamethasone as indicated. Non-irradiated skin samples were used as a control. B - Quantification of Filaggrin signal intensity from A. Means +/- SEM are represented; n=3 per biological condition.

While chronic UVA decreased filaggrin expression by 60%, GR extract restored this expression to a value close to unirradiated controls (Figure 4B). Once more, GR extract properties were comparable with a treatment with dexamethasone.

**GR extract protects dermal ECM from chronic UVA stress**

As chronic UVA irradiation affects the dermal compartment with a decrease in its density (Figure 2), we assessed type III collagen expression, a major component of the ECM that is also known to deceased with aging. Immunofluorescence staining revealed a 45% decrease in collagen III expression following chronic UVR. Consistent with the benefits of GR extract observed on the skin morphology, collagen III was protected with the rose extract, as well as with dexamethasone treatment (Figure 5).
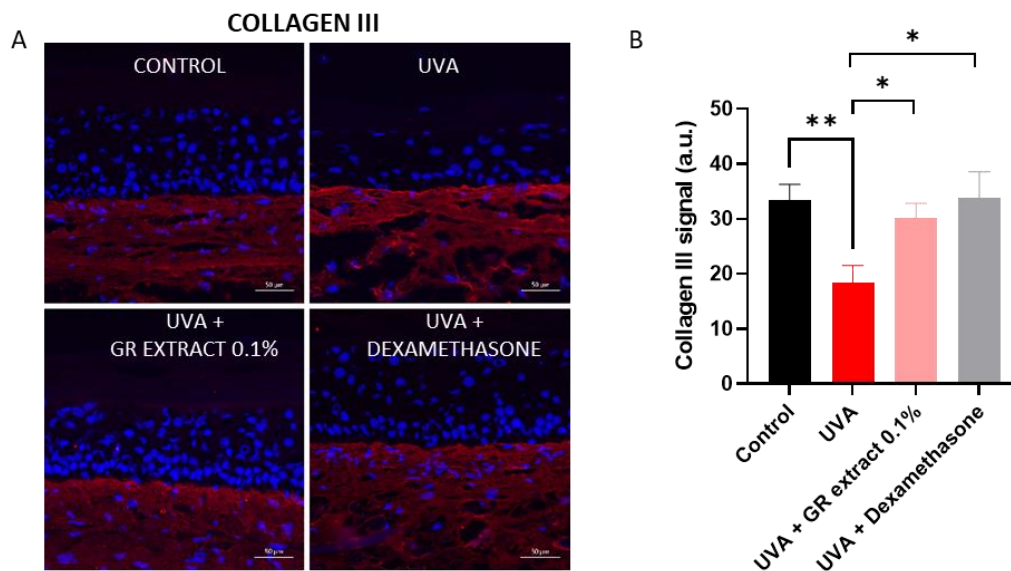


**FIGURE 5: GR extract protects 3D-printed skin from chronic UVA-induced decrease in AQP3 and Collagen III expression**
A- Representative immunostaining of 3D-bioprinted skin samples stained with an antibody against Collagen III in red and stained with DAPI in blue. Skin samples were irradiated in the presence or not of GR extract or dexamethasone as indicated. Non-irradiated skin samples were used as a control. B,D - Quantification of Collagen III signal intensity from A. Means +/- SEM are represented; n=3 per biological condition.

**Discussion**

Since it emerged the concept of inflamm'aging gained more and more attention from the scientific community. The changes in appearance and function of the skin as we age is exacerbated and

hastened by external aggressions. Our new predictive model using 3D bioprinted skin exposed to chronic UVA was able to recapitulate inflamm'aging features. We observed defects in epidermal cells differentiation, thinning of the epidermis, and an impaired barrier function. All these aspects were at least in part corrected by a treatment with dexamethasone, a known anti-inflammatory drug. Our results demonstrate that UVR triggers an inflammatory cascade within the skin, but also that this phenomenon can be prevented by our new GR extract.

We also highlighted a decreased expression of aquaporin-3 (data not shown). I was shown that the expression of aquaporin 3, which belongs to a large family of water channels, decreased with age, and favored skin dryness [10,11]. Inflamm'aging will therefore accentuate the aging-induced skin dryness. The epidermis after chronic UVR also suffered from a decreased expression of filaggrin. Filaggrin promotes the aggregation of keratin bundles, conferring keratinocytes their physical strength and contributing to epidermal hydration and barrier function. Recent work demonstrated that pollution-induced increased levels of prostaglandin E2 (PGE2) and cyclooxygenase COX2, involved in PGE2 synthesis, also decreased filaggrin expression [12]. Remarkably, both aquaporin-3 and filaggrin expression were rescued by GR extract, further supporting its noteworthy potential against inflamm'aging.

The dermal compartment was also strongly affected in our model, with a decrease in ECM density that correlates with a decreased expression of collagen III. A connection exists between an inflammatory response and ECM degradation, through the COX2/PGE2 pathway that inhibits collagen production by dermal fibroblasts [13]. GR extract preserved collagen levels and dermis density.

**Conclusion**.

Our results on these new predictive 3D bioprinted model were aligned with those obtained with *ex-vivo* and conventional *in-vitro* model, further validating the protective effects of GR extract. Altogether, our work describes a new predictive 3D bioprinted model to assess the deleterious consequences of inflamm'aging using UVA chronic inflammation. In addition, we identified GR extract as a key cosmetic ingredient to fight against inflamm'aging on all skin layers.

# References

[1] F. Tsatsou, M. Trakatelli, A. Patsatsi, K. Kalokasidis, D. Sotiriadis, Extrinsic aging, Dermato-Endocrinology. 4 (2012) 285–297. https://doi.org/10.4161/derm.22519.

[2] M.A. Farage, K.W. Miller, P. Elsner, H.I. Maibach, Intrinsic and extrinsic factors in skin ageing: a review, Int J Cosmetic Sci. 30 (2008) 87–95. https://doi.org/10.1111/j.1468-2494.2007.00415.x.

[3] H.Y. Chung, H.J. Kim, J.W. Kim, B.P. Yu, The Inflammation Hypothesis of Aging, Ann Ny Acad Sci. 928 (2001) 327–335. https://doi.org/10.1111/j.1749-6632.2001.tb05662.x.

[4] C. FRANCESCHI, M. BONAFÈ, S. VALENSIN, F. OLIVIERI, M.D. LUCA, E. OTTAVIANI, G.D. BENEDICTIS, Inflamm-aging: An Evolutionary Perspective on Immunosenescence, Ann Ny Acad Sci. 908 (2000) 244–254. https://doi.org/10.1111/j.1749-6632.2000.tb06651.x.

[5] P.U. Giacomoni, G. Rein, Textbook of Aging Skin: Skin Aging: A Generalization of the Microinflammatory Hypothesis, in: n.d.

[6] J.N. Barker, M.L. Jones, R.S. Mitra, E. Crockett-Torabe, J.C. Fantone, S.L. Kunkel, J.S. Warren, V.M. Dixit, B.J. Nickoloff, Modulation of keratinocyte-derived interleukin-8 which is chemotactic for neutrophils and T lymphocytes., Am J Pathology. 139 (1991) 869–76.

[7] T.M. Ansary, Md.R. Hossain, K. Kamiya, M. Komine, M. Ohtsuki, Inflammatory Molecules Associated with Ultraviolet Radiation-Mediated Skin Aging, Int J Mol Sci. 22 (2021) 3974. https://doi.org/10.3390/ijms22083974.

[8] S. Pillai, C. Oresajo, J. Hayward, Ultraviolet radiation and skin aging: roles of reactive oxygen species, inflammation and protease activation, and strategies for prevention of inflammation-induced matrix degradation – a review, Int J Cosmetic Sci. 27 (2005) 17–34. https://doi.org/10.1111/j.1467-2494.2004.00241.x.

[9] M. Hu, Z. Ling, X. Ren, Extracellular matrix dynamics: tracking in biological systems and their implications, J Biol Eng. 16 (2022) 13. https://doi.org/10.1186/s13036-022-00292-x.

[10] J. Li, H. Tang, X. Hu, M. Chen, H. Xie, Aquaporin-3 gene and protein expression in sun-protected human skin decreases with skin ageing, Australas J Dermatol. 51 (2010) 106–112. https://doi.org/10.1111/j.1440-0960.2010.00629.x.

[11] N. Ikarashi, R. Kon, M. Kaneko, N. Mizukami, Y. Kusunoki, K. Sugiyama, Relationship between Aging-Related Skin Dryness and Aquaporins, Int J Mol Sci. 18 (2017) 1559. https://doi.org/10.3390/ijms18071559.

[12] M. Kim, J.H. Kim, G.J. Jeong, K.Y. Park, M. Lee, S.J. Seo, Particulate matter induces pro-inflammatory cytokines via phosphorylation of p38 MAPK possibly leading to dermal inflammaging, Exp Dermatol. 28 (2019) 809–815. https://doi.org/10.1111/exd.13943.

[13] Y. Li, D. Lei, W.R. Swindell, W. Xia, S. Weng, J. Fu, C.A. Worthen, T. Okubo, A. Johnston, J.E. Gudjonsson, J.J. Voorhees, G.J. Fisher, Age-Associated Increase in Skin Fibroblast–Derived Prostaglandin E2 Contributes to Reduced Collagen Levels in Elderly Human Skin, J Invest Dermatol. 135 (2015) 2181–2188. https://doi.org/10.1038/jid.2015.157.